

# Detecting Strategic Manipulation in Distributed Optimisation of Electric Vehicle Aggregators

**Alvaro Perez-Diaz**

**Enrico Gerding**

*Electronics and Computer Science  
University of Southampton*

A.PEREZ-DIAZ@SOTON.AC.UK

EG@SOTON.AC.UK

**Frank McGroarty**

*Southampton Business School  
University of Southampton*

F.J.MCGROARTY@SOTON.AC.UK

## Abstract

Given the rapid rise of electric vehicles (EVs) worldwide, and the ambitious targets set for the near future, the management of large EV fleets must be seen as a priority. Specifically, we study a scenario where EV charging is managed through self-interested EV aggregators who compete in the day-ahead market in order to purchase the electricity needed to meet their clients' requirements. In order to reduce electricity costs and lower the impact on electricity markets, a centralised bidding coordination framework has been proposed in the literature employing a coordinator. In order to improve privacy and limit the need for the coordinator, we propose a reformulation of the coordination framework as a decentralised algorithm, employing the Alternating Direction Method of Multipliers (ADMM). However, given the self-interested nature of the aggregators, they can deviate from the algorithm in order to improve their personal utility. Hence, we study strategic manipulation of the ADMM algorithm and, in doing so, describe and analyse different attack vectors and propose a mathematical framework to quantify and detect manipulation. Moreover, this detection framework is not limited to the considered EV scenario and can be applied to general ADMM algorithms. Finally, we test the proposed decentralised coordination and manipulation detection algorithms in realistic scenarios using real market and driver data from Spain. Our empirical results show the convergence of the coordination algorithm, and that the detection algorithm accurately detects deviating behaviour in up to 96% of the cases.

## 1. Introduction

To date, there exists a world-wide fleet of more than two million electric vehicles (EVs), combining purely electrical and hybrid (International Energy Agency, 2017). Furthermore, EV sales are growing exponentially in most countries and there are targets to achieve 50 to 200 million of EVs at a global scale in the next decade (International Energy Agency, 2016). These high penetration targets aim to reduce the use of fossil fuels and improve environmental conditions. However, the transition from conventional to electric vehicles is not without challenges (Rigas, Ramchurn, & Bassiliades, 2015). Specifically, compared to traditional fuel powered vehicles, EVs present a novel and heavy strain to existing electricity networks, which will need to accommodate a new type of consumer with high demand.

In order to deal with this challenge, the last decade has seen the introduction of the concept of the EV aggregator (Kempton, Tomic, Letendre, Brooks, & Lipman, 2001): an

intermediary between a fleet of EVs and the electricity grid and markets. The aggregator is able to control the charging of its fleet, and this way informed collective decisions can be made. In contrast with individual EV operation, the much higher degree of coordination possible when a fleet is centrally managed by an aggregator offers great benefits. For example, electricity consumption to charge the fleet’s batteries can be spread over time, avoiding expensive and polluting demand peaks. In particular, in this work we focus on EV aggregators participating in day-ahead markets, in order to purchase the electricity needed to meet their clients’ energy requirements. In more detail, day-ahead markets match electricity supply and demand on an hourly basis (see Section 3), and are the main source of wholesale electricity. Here, increased electricity demand means increased prices, resulting in the so-called *price impact*, and hence it is in every market participant’s interest to avoid unnecessary demand peaks.

In this work we focus on a scenario where different EV aggregators co-exist in the same day-ahead market. These aggregators may vary in nature and size, but it is reasonable to assume that they are self-interested. Indeed, reduced electricity costs translate into more profit for the aggregator and/or more benefits for their EV fleet. In this scenario, reduced overall costs can be achieved by inter-aggregator coordination, producing more informed and optimised bidding. This coordination problem has been studied in the literature under a centralised algorithm by employing a centralised coordinator (Perez-Diaz, Gerding, & McGroarty, 2018b, 2018c). However, this centralised approach requires a trusted environment where the participating aggregators report their private information to the central coordinator. In a realistic scenario, self-interested aggregators would be reluctant to share their private business information, thus presenting an important drawback to the proposed centralised approaches.

In order to address this shortcoming, we propose a novel decentralised mechanism which allows the coordination of the EV aggregators without the need of a trusted coordinator, and without revealing their private requirement information. Specifically, we reformulate the centralised optimisation algorithm proposed by Perez-Diaz et al. (2018b) using the Alternating Direction Method of Multipliers (ADMM), which decomposes the optimisation problem into smaller problems coordinated through an aggregation step (Boyd, Parikh, Chu, Peleato, & Eckstein, 2010). Moreover, in order to provide transparency and remove the need for *trust*, the proposed algorithm can be implemented in a blockchain, using smart contracts in a very similar vein as the work by Munsing, Mather, and Moura (2017).

Although our proposed decentralised algorithm tackles the shortcoming described above, it introduces a new challenge. Specifically, in the decentralised case, the agents directly impact the computation of the optimal energy allocation, which introduces the possibility of strategic manipulation by deviating from the *vanilla* ADMM algorithm, in order to influence and modify the algorithm’s outcome. This, given that the aggregators are rational and self-interested, would happen whenever they perceive an increase in their personal utility by cheating. In order to tackle this problem, we describe how an aggregator can strategically modify its local computation in order to improve its personal gains, and how the coordinator can monitor the aggregators with a strategic manipulation detection algorithm, and penalise deviators accordingly. Specifically, we provide three attack vectors which either seek to improve an aggregator’s own energy allocation, or to incriminate another benign aggregator as deviator. We would like to remark that this issue exists in any ADMM (or variants)

decentralised optimisation scenario, where self-interested agents can try to manipulate and influence the outcome of the algorithm, and is in no way limited to EV or smart grid studies. In consequence, although we use the EV domain as a concrete example, the manipulation detection methods are generic and applicable to any ADMM setting. Note that this study on ADMM manipulation differs from existing literature as existing works only consider external attackers and noise injection, instead of self-interested insider manipulation (see Section 2.3 for more information).

In more detail, this paper makes the following contributions to the state of the art:

- We propose the first decentralised optimisation algorithm for the coordination of self-interested EV aggregator participation in day-ahead markets.
- We present the first study of strategic manipulation of the ADMM algorithm, where a self-interested agent can try to modify the algorithm’s outcome for its own benefit.
- We propose a detection algorithm to monitor the participating agents and find deviations from the vanilla ADMM algorithm.
- We present a realistic case study to empirically evaluate both the decentralised coordination and detection algorithms.

The rest of the paper is structured as follows. Section 3 introduces the considered day-ahead market and the mathematical formalism to quantify price impact. Section 4 details the considered EV aggregators and presents the proposed decentralised optimisation algorithm using ADMM. Next, a strategic manipulation study of the proposed ADMM algorithm is detailed in Section 5. Section 6 presents the proposed mathematical formalism to detect strategic manipulation of the ADMM algorithm. Next, an empirical evaluation of the proposed algorithms using real market and driver data is detailed in Section 7. Finally, we conclude in Section 8. A preliminary version of this paper was presented in (Perez-Diaz, Gerding, & McGroarty, 2018a).

## 2. Literature Review

This paper builds upon existing literature in different fields, as detailed in this section.

### 2.1 Multi-Aggregator Scenarios

A small body of the literature addresses related multi-EV aggregator scenarios, as described below. (Qi, Xu, Shen, Hu, & Song, 2014; Shao, Wang, Wang, Du, & Wang, 2016) studies the hierarchical control of EV fleets where different aggregators are coordinated by a high-level coordinator. However, in their models the aggregators are not self-interested, and instead the authors focus on accommodating grid constraints and ensuring driver satisfaction. More related to our considered scenario, Yu, Lin, Lam, and Li (2016) study a setup where a number of EV aggregators can trade energy among them in order to fix forecasting deviations, instead of purchasing the energy from the grid. Although this is shown to improve the aggregators’ energy costs, the authors do not consider price impact in their model and each aggregator performs independently. Another related work can be found in (Mukherjee & Gupta, 2017). Their work considers a scenario where several private aggregators are present

in a given city, and negotiate with each other in order to balance charging in the different limitedly available charging stations. The aim is to maximise the total number of EVs charged and the profit of the EV aggregators and their results indicate that coordinated operation improves the profit of the EV aggregators and the services offered to the drivers. Moreover, in a similar vein to our work, Wu, Shahidehpour, Alabdulwahab, and Abusorrah (2016) study a multi-aggregator day-ahead bidding scenario and apply game theory to find Nash equilibria. In more detail, each aggregator tries to categorise the other aggregators and thus forecast their day-ahead bids, and adjust their bidding accordingly. However, after introducing several approximations in order to simplify the model’s structure, the proposed model depends on a complicated optimisation algorithm and does not guarantee existence of Nash equilibria. Finally, the same scenario considered in this paper is studied from a centralised perspective in (Perez-Diaz et al., 2018b, 2018c). In these works, a number of self-interested aggregators perform coordinated bidding under the control of a centralised coordinator, and different payment mechanisms which incentivise cooperation rather than strategic manipulation are studied, using mechanism design and cooperative game theory, respectively. However, as discussed in Section 1, these centralised approaches require the aggregators to report all their private information to the coordinator, data that private entities would be reluctant to provide. In order to tackle this issue, the decentralised approach proposed in this paper removes the need for full information sharing, allowing coordination by revealing much less private information.

## 2.2 Decentralised Management in the Smart Grid

Decentralised optimisation techniques have been widely applied in smart grid and power systems scenarios. In more detail, there is a body of literature studying decentralised charging scheduling of EVs (Ardakanian, Keshav, & Rosenberg, 2014; Wen, Chen, Teng, & Member, 2012; Gan, Topcu, & Low, 2013; Ma, Callaway, & Hiskens, 2013; Le Floch, Belletti, Saxena, Bayen, & Moura, 2015; Le Floch, Belletti, & Moura, 2016). Overall, these works consider the problem of scheduling the charging of EVs in different decentralised fashions, considering each EV as a individual node in their respectively proposed algorithms. In more detail, (Ardakanian et al., 2014) focuses on physical grid constraints, considering an electricity network managed by different access points, and its interaction with a fleet of EVs. Similarly, (Gan et al., 2013; Ma et al., 2013) consider decentralised valley-filling algorithms, where the aim is to flatten demand over time, and each EV sequentially updates its own charging schedule by iterative interaction with a central utility company. In a related vein, (Wen et al., 2012) considers a decentralised algorithm which employs discrete time intervals and selects subsets of EVs to be charged at each time interval, by iterative communication between each EV and their aggregator. Finally, (Le Floch et al., 2015, 2016) considers *vehicle-to-grid* (V2G) scenarios, where the EVs are able to inject energy back to the grid when needed. Although all these works study different aspects of EV charging scheduling under decentralised algorithms, they do not consider the interaction among different self-interested aggregators, which is one of the aims of this paper.

Furthermore, decentralised algorithms have been employed in many non-EV related smart grid publications. As discussed in Section 1, an algorithm that has acquired great popularity in recent years due to its versatility and great convergence properties is ADMM

(Boyd et al., 2010). It has been employed in multitude of smart grid studies, such as power flow (Wang, Wu, & Wang, 2017; Sulc, Backhaus, & Chertkov, 2014; Peng & Low, 2014; Scott & Thiébaux, 2014) and micro-grid (Munsing et al., 2017) scenarios. However, this algorithm (or variants) has not been employed to study the decentralised coordination of self-interested aggregators.

### 2.3 Manipulation of ADMM algorithms

As described in the previous subsection, decentralised optimisation algorithms are widely used, not only in smart grid related studies, but in most technical fields. The reasons range from better scaling to large problem sizes to privacy preservation. There is, however, a gap between the introduction of such algorithms and the study of their robustness to potential manipulative/malicious attacks (Munsing & Moura, 2018). Specifically, in contrast with centralised algorithms, in the decentralised case, each node or agent participating in the algorithm will perform part of the calculations, or will transmit messages to a coordinator, hence the possibilities of cyber-attack or manipulation increase. In order to address these important issues, a few works have been published in recent years studying related topics, which will be described next. Note that we focus on ADMM algorithms, but the findings of all these studies should be generalizable to other iterative decentralised optimisation methods.

Following (Munsing & Moura, 2018), we can classify this literature based on the employed technique:

- *Round-robin techniques* (Liao & Chakraborty, 2016, 2017): these techniques seek to identify compromised nodes by replacing the coordination step of the ADMM algorithm by a round-robin detection algorithm which compares the proposals of different subsets of nodes in order to identify discrepancies. Once corrupted nodes have been identified, the coordinator switches back to the ADMM algorithm.
- *Filtering techniques* (Liao & Chakraborty, 2018): these techniques do not try to identify compromised nodes, but to employ robust statistics and outlier detection techniques in order to accurately compute the desired global quantities even in the presence of malignant data.
- *Non-linear weighting techniques* (Chen, Kar, & Moura, 2018): similarly to filtering techniques, these techniques also do not try to identify compromised nodes. Instead, they employ data from all nodes, but introduce weights to scale down the impact of suspicious nodes.
- *Convexity techniques* (Munsing & Moura, 2018): these techniques detects compromised nodes and false-data injection in convex algorithms by checking for convexity violations.

Overall, these works focus on cyber-security, *i.e.* the effects of external attacks which compromise an internal node (a participant in the ADMM algorithm). Moreover, the papers discussed above focus on random noise injection by a malignant agent, which prevents the algorithm from converging. In contrast, in this work, we study strategic manipulation of the

ADMM algorithm by internal self-interested agents. In more detail, rather than considering external malignant attackers, we consider algorithm participants that want to achieve more beneficial outcomes for themselves, even if this is in detriment of the other participants, and deviate from the vanilla ADMM algorithm in order to do so. This differs from these existing works in two aspects: (i) the algorithm can still converge to a stable outcome, (ii) the manipulating agents will use clever cheating techniques, as injecting random noise will not be beneficial for them.

### 3. The Day-Ahead Market

This section details the day-ahead market structure considered in this paper and present in most countries. Moreover, we discuss how to quantify the price impact of buy orders (electricity demand), which is an important aspect of our work. The exposition in this section follows (Perez-Diaz et al., 2018b, 2018c).

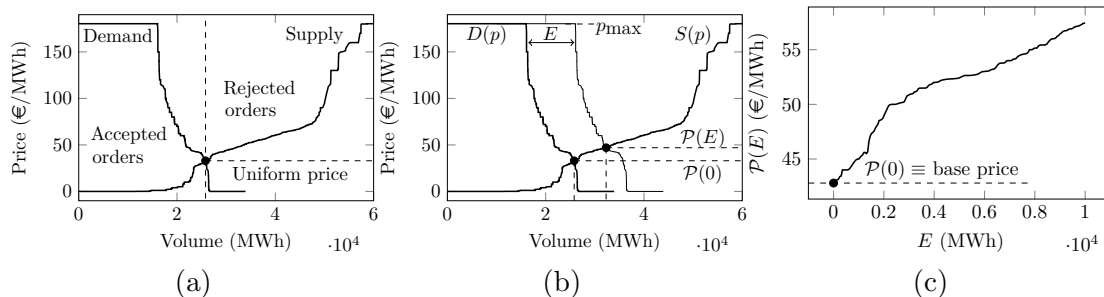


Figure 1: (a) Aggregated supply and demand curves, and market clearing mechanism. (b) Price impact of a buy order with volume  $E$  and maximum price  $p_{\max}$ . (c) Final price function  $\mathcal{P}(E)$ . Source: OMIE, 01/11/2016, 11<sup>th</sup> hour.

Day-ahead markets divide each day into 24 hourly slots, each running a separate uniform-priced double-sided auction. Before closure time (usually noon) on day  $D$ , bids and offers for each hourly slot of day  $D + 1$  must be submitted to the market. Then, a matching algorithm determines the accepted bids and offers, and establishes an hourly uniform price using marginal pricing, this is, the price of the intersection between supply and demand.

Bids (buy orders) and offers (sell orders) for each hourly slot are quantity-price pairs. For bids (offers), the price represents the highest (lowest) price the participant is willing to pay (sell for). As is common in most markets, we define a minimum price  $p_{\min} = 0$  and some maximum price,  $p_{\max}$ . After closure time, the auctioneer aggregates all buy and sell orders, by high-price and low-price priorities, respectively. This generates the aggregated demand and supply curves, and their intersection determines the accepted orders and the resulting uniform price, as depicted in Fig. 1 (a).

Clearly, the arrival of a new buy order pushes the clearing price up if it gets accepted (*i.e.* if it lies towards the left-hand side of the intersection). Fig. 1 (b) illustrates the effect of a new buy order with quantity  $E$  placed at price  $p_{\max}$ . The price increase (price impact) depends on the new order's price and quantity, and on the supply and demand curves. Price impact is an essential market characteristic associated with large market participants, and

careful managing is required to avoid pushing prices up unnecessarily. Price impact has been studied in the electricity markets literature by employing residual curves (Herranz, Muñoz San Roque, Villar, & Campos, 2012; Perez-Diaz et al., 2018b, 2018c, 2018a), which are detailed below.

Employing standard notation, for any given hour  $t$ , let  $D_t(p)$  and  $S_t(p)$  be the aggregated demand and supply curves respectively, as a function of price,  $p$ . The residual supply curve is defined as  $R_t(p) = S_t(p) - D_t(p) = E$ , and represents the amount of energy,  $E$ , an agent could bid for while maintaining a clearing price  $p$ . Conversely, the clearing price when bidding a quantity  $E$  is given by  $p = R_t^{-1}(E)$ . Introducing the notation  $\mathcal{P}_t(E) = R_t^{-1}(E)$ , the clearing price when the new agent bids an amount  $E$  is  $p = \mathcal{P}_t(E)$ , and the price impact  $\Delta p$  of this order is given by  $\Delta p = \mathcal{P}_t(E) - \mathcal{P}_t(0)$ , where  $\mathcal{P}_t(0)$  represents the *base price* at hour  $t$ , i.e. the price without the agent’s new bid. This formalism is depicted in Figs. 1 (b) and (c).

We are now ready to introduce the EV aggregator model considered in this paper and the optimal day-ahead bidding algorithm.

## 4. Optimal Multi-EV Aggregator Participation in the Day-Ahead Market

As discussed in Section 1, an EV aggregator is responsible for the charging of a fleet of EVs and, to this end, purchases the required electricity from the day-ahead market (see Section 3). We will start by describing the considered aggregator structure and operation. Then, we will describe the optimal bidding algorithm proposed in (Perez-Diaz et al., 2018b, 2018c, 2018a) and how it can be used to optimise the bidding of a group of EV aggregators with a central coordinator. Finally, we will decompose this centralised algorithm into a decentralised optimisation algorithm by using the Alternating Direction Method of Multipliers (ADMM), as discussed in Section 1.

### 4.1 EV Aggregator Model

In our model, following (Bessa, Matos, Soares, & Lopes, 2012; Perez-Diaz et al., 2018b, 2018c, 2018a), EVs arrive and depart dynamically over time. When an EV  $i$  arrives to the charging point, it communicates the desired departure time,  $t_d^i$ , and desired state of charge at departure,  $\text{SoC}_d^i$ , to the aggregator. We assume that arrival time and state of charge,  $t_0^i$  and  $\text{SoC}_0^i$  can be automatically inferred by the aggregator. Each EV has a maximum charging speed,  $P_{\max}^i$  in kW, which depends on two factors: the available physical infrastructure, and the EV’s battery. The charging schedule of the EV is then left at the aggregator’s discretion, which can choose when to perform the charging while guaranteeing the desired state of charge by departure time. This flexibility allows charging the battery in an informed way, rather than randomly, or at arrival, providing cheaper electricity costs.

Due to the nature of the day-ahead market, electricity bids need to be placed between 12 and 36 hours before delivery time (assuming market closure at noon, see Section 3). This requires the market participants to forecast their electricity needs, as described next, and bid accordingly.

Following (Bessa et al., 2012; Perez-Diaz et al., 2018b, 2018c, 2018a), we model the requirements of an EV  $i$  by employing two vectors with 24 entries each,  $\mathbf{r}^{\min,i}$  and  $\mathbf{r}^{\max,i}$ . Specifically,  $r_t^{\min,i}$  is the amount of energy needed at hour  $t$  assuming charging has been

left for the last possible moment and that the charging requirements need to be fulfilled. Conversely,  $r_t^{\max,i}$  is the amount of energy needed at hour  $t$  assuming charging starts as soon as possible. For example, consider an EV arriving at 3pm, stating 9pm departure time and 8kWh charging needs with  $P_{\max} = 3\text{kW}$ . Then,  $\mathbf{r}^{\min,i}$  would be as specified in Table 1. Specifically, if 6pm is reached with no charging done, at least 2kW of energy needs to be charged between 6-7pm in order to fulfil the EV driver requirements. The same applies with 3kW between 7-8pm and 8-9pm. Similarly, for the same scenario, the requirement vector  $\mathbf{r}^{\max,i}$  would be as specified in Table 2.

Then, in order to provide mathematical tractability, two global energy requirement vectors,  $\mathbf{R}^{\min}$  and  $\mathbf{R}^{\max}$ , can be obtained by summing the hourly requirements of all the EVs associated to the particular aggregator, *i.e.*  $R_t^{\min} = \sum_{i=1}^N r_t^{\min,i}$  and  $R_t^{\max} = \sum_{i=1}^N r_t^{\max,i}$ . Note that these aggregated constraints do not exactly capture the individual requirements of each EV, but have been widely employed in the literature (Bessa et al., 2012; Bessa & Matos, 2013a, 2013b; Gonzalez Vaya & Andersson, 2015; Perez-Diaz et al., 2018b, 2018c, 2018a). The reasons are the fact that considering constraints for each individual EV renders the problem unfeasible with moderate problem sizes, and the fact that bidding uses day-ahead price and energy requirements forecasts, which will not be exact anyway.

We will denote the quantities that need to be forecasted with a hat: hourly energy requirements,  $\hat{R}_t^{\min}$  and  $\hat{R}_t^{\max}$ , hourly number of available EVs,  $\hat{N}_t$ , and hourly price impact functions,  $\hat{P}_t$ .

$r_3^{\min,i}$	$r_4^{\min,i}$	$r_5^{\min,i}$	$r_6^{\min,i}$	$r_7^{\min,i}$	$r_8^{\min,i}$	$r_9^{\min,i}$
0	0	0	2	3	3	0

Table 1: Example of requirement vector  $\mathbf{r}^{\min,i}$

$r_3^{\max,i}$	$r_4^{\max,i}$	$r_5^{\max,i}$	$r_6^{\max,i}$	$r_7^{\max,i}$	$r_8^{\max,i}$	$r_9^{\max,i}$
3	3	2	0	0	0	0

Table 2: Example of requirement vector  $\mathbf{r}^{\max,i}$

## 4.2 Optimal Day-Ahead Bidding Algorithm

Now that the day-ahead and EV aggregator models have been detailed, we are ready to present the optimal day-ahead bidding algorithm. The algorithm is from (Perez-Diaz et al., 2018b, 2018c, 2018a) and reproduced here for convenience. The mathematical problem is defined as follows: given an EV aggregator’s forecasted requirements and price impact functions, find the optimal distribution of energy quantities to bid across the 24 hourly slots of the next day,  $\mathbf{E} = (E_0, \dots, E_{23})$ , in order to satisfy its clients’ charging needs while minimising the total cost of the purchased energy. We assume that the agent’s bids are set at maximum price,  $p_{\max}$ , in order to guarantee execution. Hence only bidding hours and quantities need to be decided.

As discussed in (Perez-Diaz et al., 2018b), and in order to avoid a complex minimisation landscape with multiple minima, the forecasted hourly price impact functions  $\hat{P}_t$  (see Sections 3 and 4.1) are approximated by quadratic convex functions. Specifically, they are



given by  $\hat{\mathcal{P}}_t^{\text{convex}} = a_t E_t^2 + b_t E_t + \hat{\mathcal{P}}_t(0)$ , where all the coefficients  $a_t$  are restricted to be positive. Formally, the optimisation algorithm is given by Eqs. (1a), (1b), (1c), (1d). In more detail, the objective function (1a) minimizes the total cost of the purchased energy. The constraints guarantee that the amount of purchased energy is enough to satisfy the forecasted demand (1b), that it is not purchased before the forecasted arrival of the EVs (1c) and that the energy purchased at each hour is not greater than the amount that the aggregator is able to charge at the given hour, based on the forecasted number of available vehicles (the aggregator cannot store energy). It is worth noting that the number of constraints is always 72, independent on the fleet size. Also, given the convexity of the problem, there exists a unique global minimum, which we are guaranteed to find.

$$\min_{\{E_t\}} \sum_t \hat{\mathcal{P}}_t(E_t) \cdot E_t \quad (1a)$$

$$\sum_{j=0}^t E_j \geq \sum_{j=0}^t \hat{R}_j^{\min}, \quad \forall t = 0, \dots, 23 \quad (1b)$$

$$\sum_{j=0}^t E_j \leq \sum_{j=0}^t \hat{R}_j^{\max}, \quad \forall t = 0, \dots, 23 \quad (1c)$$

$$E_t / \Delta t \leq \hat{N}_t P_{\max}, \quad \forall t = 0, \dots, 23 \quad (1d)$$

### 4.3 Centralised Joint Bidding

The bidding algorithm detailed in the previous section for a single aggregator can be extended to perform joint bidding, where a coordinator collects the requirements of a number of independent aggregators and applies the optimisation algorithm globally. In more detail, consider a set of  $n$  EV aggregators. Then, following (Perez-Diaz et al., 2018b, 2018c, 2018a) and overloading the variable  $i$ , let  $\hat{R}_t^{\min,i}$  and  $\hat{R}_t^{\max,i}$  be aggregator  $i$ 's forecasted energy requirements for hour  $t$ , and  $\hat{N}_t^i$  the number of available EVs from aggregator  $i$ , as specified in Section 4.2. The combined requirements of all the aggregators are then:

$$\hat{R}_t^{\min} = \sum_{i=1}^n \hat{R}_t^{\min,i} \quad (2) \quad \hat{R}_t^{\max} = \sum_{i=1}^n \hat{R}_t^{\max,i} \quad (3) \quad \hat{N}_t = \sum_{i=1}^n \hat{N}_t^i \quad (4)$$

To find the optimal global energy bids, the bidding optimisation algorithm given by Eqs. (1a), (1b), (1c), (1d) can be applied with constraints given by the combined requirements (2), (3) and (4). This will result in obtaining a global day-ahead energy volume  $E_t$  for each hour  $t$ , which can be then distributed among the  $n$  aggregators.

The redistribution mechanism is defined in (Perez-Diaz et al., 2018b), and allocates an hourly energy schedule to each participating aggregator after obtaining a global energy schedule as detailed above. The redistribution problem is as follows. Letting  $E_t^i$  be the amount of energy allocated to EV aggregator  $i$  at time  $t$ , we need to find  $E_t^i$  for  $t = 0, \dots, 23$

and  $i = 1, \dots, n$  satisfying the following constraints:

$$\sum_{j=0}^t E_j^i \geq \sum_{j=0}^t \hat{R}_j^{\min}, \forall t = 0, \dots, 23; \forall i = 1, \dots, n \quad (5a)$$

$$\sum_{j=0}^t E_j^i \leq \sum_{j=0}^t \hat{R}_j^{\max}, \forall t = 0, \dots, 23; \forall i = 1, \dots, n \quad (5b)$$

$$E_t^i / \Delta t \leq \hat{N}_t^i P_{\max}, \forall t = 0, \dots, 23; \forall i = 1, \dots, n \quad (5c)$$

$$\sum_{i=1}^n E_t^i = E_t, \forall t = 0, \dots, 23 \quad (5d)$$

In this constraint satisfaction problem, Eqs. (5a), (5b), (5c) ensure that each EV aggregator has enough energy to satisfy its requirements, no more, no less, for each hour. Eq. (5d) makes sure the sums of the allocated hourly energies add up to the available global energy.

#### 4.4 Decentralised Optimisation Algorithm

We are now ready to introduce the novel decentralised optimisation algorithm based on ADMM (Boyd et al., 2010). Specifically, our goal is to reformulate the optimisation problems given by Eqs. (1a), (1b), (1c), (5a), (5b), (5c) as an iterative decentralised algorithm, where each EV aggregator solves a local optimisation problem. The solutions to each local problem are coordinated by a global *consensus* step, and this procedure is iterated. *Consensus* refers to the fact that, asymptotically, all the local variables will coincide. This type of algorithm is appropriate in our setting for several reasons: (i) given that our problem is convex, it is guaranteed to converge to the global optimum (Boyd et al., 2010); (ii) it enables coordination without the aggregators revealing their energy requirements, *i.e.*  $\mathbf{R}^{\min}$  and  $\mathbf{R}^{\max}$ ; (iii) it is particularly well suited for blockchain implementation, providing transparency and anti-tampering guarantees (Perez-Diaz et al., 2018a; Munsing et al., 2017).

Following the notation introduced in Section 4.3, recall that  $\mathbf{E}^i = (E_0^i, \dots, E_{23}^i)$  denotes the energy schedule for aggregator  $i$ . Moreover, let  $\mathbf{E} = (\mathbf{E}^1, \dots, \mathbf{E}^n)$  be the joint vector encapsulating each individual energy schedule, and  $\mathbf{E}^{\text{glob}} = (E_1^{\text{glob}}, \dots, E_{23}^{\text{glob}})$  be a vector such that  $E_t^{\text{glob}} = \sum_{i=1}^n E_t^i$ . We can now rewrite Eq. (1a) as:

$$\begin{aligned} \min_{\mathbf{E}^{\text{glob}}} \sum_{t=0}^{23} \hat{\mathcal{P}}_t(E_t^{\text{glob}}) \cdot E_t^{\text{glob}} &= \min_{\mathbf{E}} \sum_{t=0}^{23} \left[ \hat{\mathcal{P}}_t \left( \sum_{i=1}^n E_t^i \right) \cdot \sum_{i=1}^n E_t^i \right] = \\ &= \min_{\mathbf{E}} \sum_{i=1}^n \left[ \sum_{t=0}^{23} \left( E_t^i \cdot \hat{\mathcal{P}}_t \left( \sum_{j=1}^n E_t^j \right) \right) \right] \end{aligned} \quad (6)$$

This way the objective function is expressed as a sum of  $n$  terms, as required by the ADMM formulation (Boyd et al., 2010). Note that, given that the price impact of each aggregator affects everybody else, we cannot separate Eq. (6) in the variable  $i$ , *i.e.* the equation is

coupled and the sum's terms cannot be independently distributed among the aggregators. This type of problem is suited to be formulated as a *global variable consensus problem* (Boyd et al., 2010), which works as follows. Consider a minimisation problem in the following form:

$$\min_{\mathbf{x}} \sum_{i=1}^n f_i(\mathbf{x})$$

where the goal is that each term in the sum can be handled independently. In the cases where the variable  $\mathbf{x}$  is not separable in  $i$ , *local* variables  $\mathbf{x}^i$  and a *global* variable  $\mathbf{z}$  can be introduced, rewriting the problem as:

$$\min_{\{\mathbf{x}^i\}} \sum_{i=1}^n f_i(\mathbf{x}^i)$$

$$\text{subject to: } \mathbf{x}^i - \mathbf{z} = 0, \forall i = 1, \dots, n$$

As mentioned above, the problem constraints require all local variables to agree with each other and with the global variable. This way, global consensus on the solution is achieved. Also, note that any individual constraints can be embedded into each  $f_i$ .

In a similar vein and focusing on our scenario, let  $\mathbf{E}$  and  $\mathbf{E}^{(i)}$  be the global and local variables respectively, each of which comprises a vector with dimension  $24n$  *i.e.*  $\mathbf{E}^{(i)} = (\mathbf{E}^{(i),1}, \dots, \mathbf{E}^{(i),n})$  and  $\mathbf{E}^{(i),j} = (E_0^{(i),j}, \dots, E_{23}^{(i),j})$ . Following Eq. (6), the functions  $f_i$  are given by:

$$f_i(\mathbf{E}^{(i)}) = \begin{cases} \sum_{t=0}^{23} [E_t^{(i),i} \cdot \hat{\mathcal{P}}_t(\sum_{j=1}^n E_t^{(i),j})], & \text{if constraints (1b), (1c), (1d) are met by } \mathbf{E}^{(i),i} \\ \infty & \text{, otherwise} \end{cases}$$

The resulting ADMM algorithm is then given by the following iterative equations:

$$\mathbf{E}_{[k+1]}^{(i)} = \arg \min_{\mathbf{E}'} (f_i(\mathbf{E}') + \boldsymbol{\xi}_{[k]}^{(i)T} (\mathbf{E}' - \mathbf{E}_{[k]}) + \frac{\rho}{2} \|\mathbf{E}' - \mathbf{E}_{[k]}\|_2^2) \quad (7a)$$

$$\mathbf{E}_{[k+1]} = \frac{1}{n} \sum_{i=1}^n \left( \mathbf{E}_{[k+1]}^{(i)} + \frac{1}{\rho} \boldsymbol{\xi}_{[k]}^{(i)} \right) \quad (7b)$$

$$\boldsymbol{\xi}_{[k+1]}^{(i)} = \boldsymbol{\xi}_{[k]}^{(i)} + \rho \left( \mathbf{E}_{[k+1]}^{(i)} - \mathbf{E}_{[k+1]} \right) \quad (7c)$$

where the subscript  $[k]$  denotes iteration number, and  $\boldsymbol{\xi}$  and  $\rho$  are the dual variable and the augmented Lagrangian parameter, respectively (Boyd et al., 2010). Intuitively,  $\rho$  controls the trade-off between each aggregator solving its own local problem, and achieving global consensus (not necessarily to a minimum point). In more detail, if  $\rho$  is set too high, the algorithm forces consensus *too much*, resulting in very slow convergence. Conversely, if  $\rho$  is set too small, each aggregator solves its local problem and consensus is not reached. Examples of this are presented in Section 7.2.

Given this, the iterative algorithm works as follows: first, each EV aggregator solves their local problem, Eq. (7a), and update their local copy of the energy schedule,  $\mathbf{E}^{(i)}$ . Then, an

aggregation step, Eq. (7b), collects all the local solutions proposed by each aggregator and updates the global energy schedule,  $\mathbf{E}$ , reporting this vector back to all the aggregators. Lastly, each aggregator updates their local copy of the dual variable,  $\boldsymbol{\xi}^{(i)}$ , as per Eq. (7c) and proceeds to the new iteration.

This iterative process is stopped when the primal and dual residuals reach some user-specified tolerances,  $\epsilon_{\text{pri}}$  and  $\epsilon_{\text{dual}}$  (Boyd et al., 2010; Munsing et al., 2017). Specifically, the primal residual is denoted by  $\mathbf{r}_{[k]} = (\mathbf{r}_{[k]}^1, \dots, \mathbf{r}_{[k]}^n)$ , where  $\mathbf{r}_{[k]}^i = \mathbf{E}_{[k]}^{(i)} - \mathbf{E}_{[k]}$ . Similarly, the dual residual is given by  $\mathbf{s}_{[k]} = \mathbf{E}_{[k]} - \mathbf{E}_{[k-1]}$ . The stopping criterion then takes the following form:

$$\|\mathbf{r}_{[k]}\|_2^2 \leq \epsilon_{\text{pri}} \quad (8a)$$

$$\|\mathbf{s}_{[k]}\|_2^2 \leq \epsilon_{\text{dual}} \quad (8b)$$

and the algorithm stops when both conditions have been met.

This concludes the exposition of the novel decentralised algorithm, which will be empirically tested in Section 7.2. We are now ready to study how the algorithm could be manipulated by a self-interested agent, and how this can be detected.

## 5. Strategic Manipulation of the ADMM Algorithm

The ADMM-based algorithm described in the previous section has nice convergence properties and (asymptotically) reaches the global optimum for suitable values of  $\rho$  (Boyd et al., 2010). However, this requires every participating agent to run the algorithm faithfully. In our case, where agents are assumed to be self-interested, an aggregator could deviate from their assigned local algorithm and/or misreport their local solutions if this improves their allocation. Therefore, in this section we focus on the strategic manipulation of our proposed ADMM algorithm, Eqs. (7a), (7b), (7c), and we will show how a misbehaving aggregator can significantly affect the algorithm's outcome. Note that we do not look at all possible manipulation vectors, as this is not feasible, but instead focus on three specific types of manipulation, the so-called *proportional*, *shift* and *adversarial* attacks, selected for their effectiveness and intuitive behaviour.

### 5.1 Proportional Attack

In this type of manipulation, the deviating aggregator  $i$  runs its local optimisation problem, Eq. (7b), but changes its local schedule allocation for another aggregator  $j$ ,  $\mathbf{E}^{(i),j}$ , by a factor  $\lambda \in [0, 1]$ , which indicates the *strength* of the attack. Formally,  $\mathbf{E}_{[k+1]}^{(i)}$  is obtained from Eq. 7b, and then modified as:

$$\hat{\mathbf{E}}_{[k+1]}^{(i),j} = \mathbf{E}_{[k+1]}^{(i),j} \cdot (1 - \lambda) \quad (9)$$

This form of manipulation can be used to force the competing aggregator  $j$  out of aggregator  $i$ 's desired schedule. Obviously, this attack is very naive and can lower the total amount of electricity allocated to the attacked aggregator  $j$ , making it relatively easy to detect as the total amount of energy allocated to aggregator  $j$  will not satisfy its requirements. However, in many cases, it effectively alters the energy schedule of aggregator

$j$  without actually reducing the total amount of energy. In this case, as the total amount of energy allocated to aggregator  $j$  is not artificially too small, this deviating behaviour is not obvious to detect.

## 5.2 Shift Attack

In this more sophisticated attack, aggregator  $i$  *shifts* the energy allocation of aggregator  $j$  to more expensive hours (or outside aggregator  $i$ 's preferred hours) without altering the energy quantities. This allows the deviating aggregator  $i$  to obtain its desired energy schedule at reduced prices, as the price impact of aggregator  $j$  on the desired hours is eliminated. In this work and without loss of generality, we will focus on a particular case where the deviating aggregator splits the energy schedule of the attacked aggregator  $j$  by its mid-hour, and then shifts both halves outwards by a number of hours  $\mu = 1, 2, \dots$ , as depicted in Fig. 2. This is motivated by the fact that, normally, the cheapest prices lie somewhat in the middle hours of the day.

In more detail, let  $t^*$  be the median hour with non-negative energy allocation for agent  $j$ ,  $\mathbf{E}_{[k+1]}^{(i),j}$ . Then, given  $\mathbf{E}_{[k+1]}^{(i)}$  from Eq. 7b, the allocation of aggregator  $j$  is modified as follows:

$$\hat{\mathbf{E}}_{[k+1], t}^{(i),j} = \begin{cases} 0, & \text{if } t \in [[t^*] - \mu, [t^*]] \\ 0, & \text{if } t \in [[t^*], [t^*] + \mu] \\ E_{[k+1], t+1}^{(i),j}, & \text{if } t \leq t^* - \mu \\ E_{[k+1], t-1}^{(i),j}, & \text{if } t > t^* + \mu \end{cases} \quad (10)$$

Note that in the mathematical formulation presented in Eq. 10 the allocation can be pushed beyond the 24h day interval for large values of  $\mu$ , but this does not happen for the range of values employed in the empirical evaluation described in Section 7.

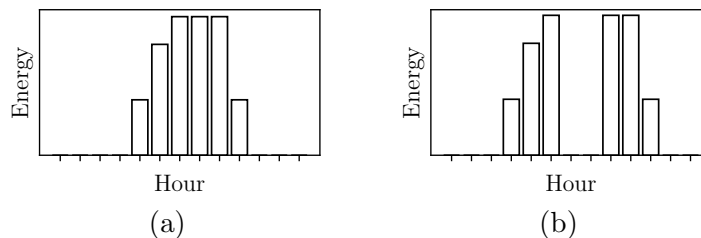


Figure 2: (a) Truthful allocation from aggregator  $i$  to aggregator  $j$  following Eq. 7b,  $\mathbf{E}_{[k+1]}^{(i),j}$ .  
 (b) Attacked  $\hat{\mathbf{E}}_{[k+1]}^{(i),j}$  employing a shift attack with  $\mu = 1$  as given by Eq. 10.

## 5.3 Adversarial Attack

This last type of attack we consider is different from the two previously described ones, as the deviating aggregator  $i$  does not directly seek to manipulate another aggregator's allocation. Instead, it will try to make a incriminate a benign aggregator  $j$  to make it appear as a deviator, hoping it will be a false positive of the manipulation detection algorithm and

penalised accordingly. Depending on the imposed penalty, this can consist on banning aggregator  $j$ 's participation on the current trading day, thus benefiting aggregator  $i$  as price impact is reduced. Otherwise, this can be seen as a purely malignant adversarial attack.

This attack can be performed by proposing a schedule for aggregator  $j$ ,  $\mathbf{E}_{[k+1], t}^{(i),j}$ , closer to the allocation of aggregator  $j$  to itself in the previous round,  $\mathbf{E}_{[k]}^{(j),j}$ . Hence aggregator  $j$  appears to deviate from the algorithm as it breaks the balance in aggregators  $i$ - $j$  interaction. This will become clear in Section 6.1 where we describe our proposed method to quantify manipulation.

This attack can be parametrised by a parameter  $\lambda \in [0, 1]$  which determines a linear combination between the schedule proposed by aggregator  $j$  to itself, and the schedule allocated by aggregator  $i$  to  $j$  as a result of Eq. (7a). Formally, given  $\mathbf{E}_{[k+1]}^{(i),j}$  from Eq. 7b, modify the allocation to aggregator  $j$  as follows:

$$\hat{\mathbf{E}}_{[k+1]}^{(i),j} = \mathbf{E}_{[k+1]}^{(i),j} \cdot (1 - \lambda) + \mathbf{E}_{[k]}^{(j),j} \cdot \lambda$$

In more detail, an attack with parameter  $\lambda = 1$  proposes an allocation to aggregator  $j$  equal to what  $j$  proposed for itself in the previous round. This is likely to be beneficial for aggregator  $j$ 's schedule, as it will contribute towards maintaining the more favourable schedules characteristic of early rounds before convergence. However, as will be detailed in Section 6.1, this will make benign aggregator  $j$  seem a deviator, with the subsequent penalty. Conversely, as  $\lambda$  tends to zero, we recover the benign ADMM algorithm.

#### 5.4 ADMM Convergence under Strategic Manipulation

As described in Section 2, existing works in the literature focus on attacks to the ADMM algorithm that seek to destabilise it and prevent its convergence. While this can be beneficial for a malignant attacker whose objective is to prevent the algorithm's operation, it is not necessarily so in our case with self-interested participants. In more detail, a given EV aggregator may want to completely prevent coordinated bidding by interrupting convergence of the proposed coordination algorithm, but most likely it will try to improve its own allocation by manipulating the algorithm in a *subtle* way that goes unnoticed. Therefore, although in both cases deviating behaviour needs to be detected and stopped, we will now show several examples of the effects of three proposed attack vectors in terms of the convergence of the ADMM algorithm.

In Figure 3 we show a scenario with three aggregators, where one deviating aggregator performs a proportional attack with strength  $\lambda = 0.83$  against another aggregator. We can see that the total cost is actually increased, while both the primal and dual residuals are very close to the *vanilla* case, where all aggregators are benign. This effectively means that the manipulating aggregator is able to actually alter the outcome of the algorithm without affecting convergence, thus going unnoticed if care is not taken.

Next, in Figure 4, we present another scenario with three aggregators, where one deviating aggregator performs a shift attack with parameter  $\mu = 2$  against another aggregator. We can see that, in this case, although the outcome has changed resulting in significantly higher total costs, the primal residuals do not converge towards zero, thus the algorithm will

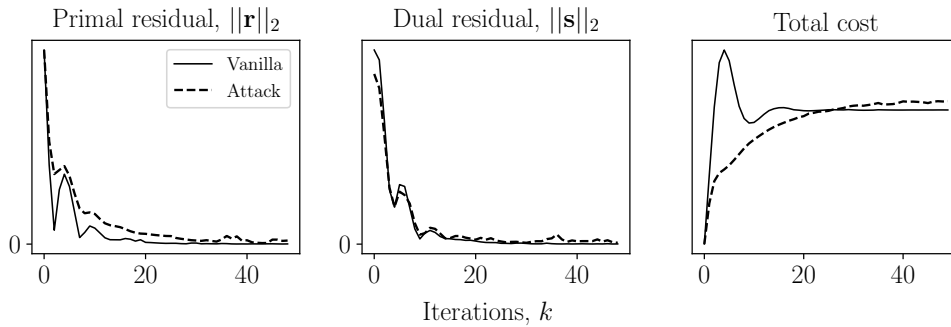


Figure 3: Proportional attack to a single aggregator with  $\lambda = 0.83$  in a scenario with three aggregators.

not converge and it is easy to detect that manipulation is occurring by some agent. However, as mentioned earlier, the manipulating aggregator needs to be identified and stopped in order for the algorithm to successfully produce an energy schedule for the rest of the benign aggregators.

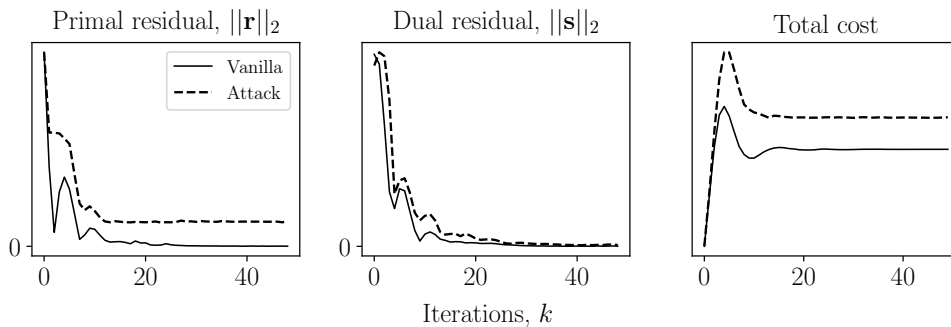


Figure 4: Shift attack to a single aggregator with  $\mu = 2$  in a scenario with three aggregators.

Lastly, in Figure 5, we present the outcome of a scenario with four aggregators where one deviating aggregator performs an adversarial attack with parameter  $\lambda = 0.83$  against another aggregator. In this case, all residuals and outcome are pretty much unaffected, and the algorithm converges normally. However, the attacked aggregator (recall that in this attack type the attacker tries to cheat the detection algorithm into wrongly classifying the attacked aggregator as a deviator) will be falsely classified as deviator if the detection algorithm is not designed carefully. This will become clear in Section 6.

We are now ready to study how strategic manipulation can be detected.

## 6. Detecting Manipulation

In this section, we detail a mathematical framework for quantifying the influence of a given ADMM participant, *i.e.* an aggregator, onto the rest of participants. The aim is to be able to detect outliers that are symptom of strategic manipulation in the system. This

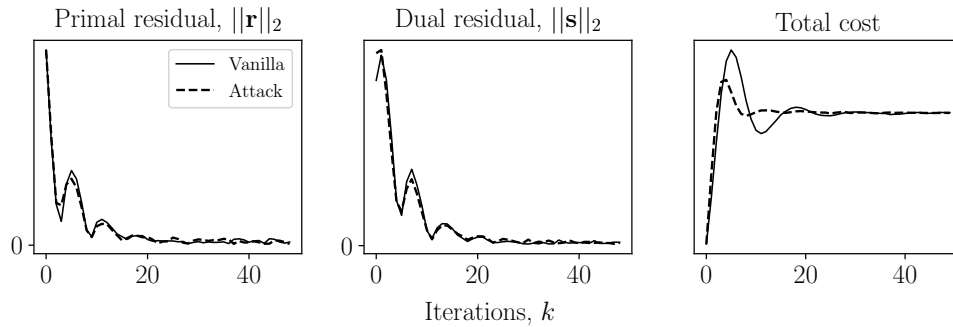


Figure 5: Adversarial attack to a single aggregator with  $\lambda = 0.83$  in a scenario with four aggregators.

framework is general, and can be applied to any ADMM (or variant) scenario, although we focus on our particular case for easier exposition.

### 6.1 Quantifying Manipulation

The basic idea is that any group of aggregators with overlapping energy requirements should influence each other’s schedules with *similar* intensity. If a particular aggregator  $i$  is self-interested and wants to improve its allocation by deviating from the ADMM algorithm, it will exert a heavier influence onto its competitors’ allocations. Conversely, as happens in the adversarial attack detailed in Section 5.3, an aggregator that tries to wrongly flag another benign aggregator as deviator would exert too little influence.

A key point is that each aggregator  $i$  produces a (local) proposed schedule for all the  $n$  participating aggregators. Formally, following the notation from Section 4.4:

$$\mathbf{E}_{[k+1]}^{(i)} = \left( \mathbf{E}_{[k+1]}^{(i),1}, \dots, \mathbf{E}_{[k+1]}^{(i),n} \right)$$

Hence, this local solution proposed by aggregator  $i$  contains its own schedule,  $\mathbf{E}_{[k+1]}^{(i),i}$ , and all the schedules for all the other participants,  $\mathbf{E}_{[k+1]}^{(i),j}$  for  $j \neq i$ . We assume that each aggregator, benign or deviator, is truthful about their own allocations in their proposed local solutions. The reason for this is that every aggregator wants the best energy schedule given their requirements, and would gain no benefit from lying about this. This suggests that a manipulating agent would only try to modify the competitors’ allocations in order to reduce overlapping. Consequently, we can reasonable assume these self-allocations to be truthful, and analyse how each aggregator affects its competitors’ allocations in successive rounds. Without loss of generality, we assume that the deviating behaviour starts from the second ADMM round, when every aggregator has seen the proposals from each aggregator. This allows us to focus on the first two iterations ( $k = 0, 1$ ) for ease of exposition.

Formally, let  $d$  be a square matrix of dimension  $n$ , the *difference matrix*, storing how much each aggregator affects its competitors’ self-proposed allocations. In more detail, every  $i, j$  entry quantifies how much aggregator  $i$  modifies the self-assigned schedule of agent  $j$ , and is given by:

$$d^{i,j} = \left\| E_{[1]}^{(i),j} - E_{[0]}^{(j),j} \right\|$$



As mentioned above, we expect benign aggregators to affect each other’s schedules in a similar way, but aggregator size significantly affects this. More precisely, there are natural magnitude deviations in  $d^{i,j}$  and  $d^{j,i}$  when the sizes of the benign aggregators  $i$  and  $j$  differ.

In order to overcome this issue, we normalise the matrix  $d$  employing the total amount of energy allocated by each aggregator to itself, as a proxy to unknown aggregator size. Thus we can write:

$$\text{size}_i = \sum_{t=0}^{23} E_{[0]}^{(i),i}$$

and the proportion of the size of aggregator  $i$  among the whole group of aggregators is given by:

$$p_i = \frac{\text{size}_i}{\sum_j \text{size}_j}$$

Then, the *normalised difference matrix*,  $\bar{d}$ , is given by:

$$\bar{d}^{i,j} = \|E_{[1]}^{(i),j} - E_{[0]}^{(j),j}\| \cdot \frac{\sqrt{p_i}}{\text{size}_i + \text{size}_j} \quad (11)$$

The employed scaling was chosen as it empirically *flattens* the entries of the matrix  $\bar{d}$  corresponding to benign aggregators, eliminating most of the dependence on aggregator size. This is further discussed with numerical examples in Section 7.3.

Lastly, we assume that  $n - 1$  aggregators are benign and only one of them can potentially be a deviator. This is motivated by the fact that, with a perfect detection algorithm, there exists a Nash equilibrium in which no-one wants to deviate. Note that the proposed detection algorithm, which we are now ready to introduce, could be extended to deal with a general case.

## 6.2 Detecting Manipulation

The overall idea is to be able to detect deviating aggregators in order to penalise and discourage manipulation. As it is usually the case in stochastic complex environments, the aim here is to reduce false positives and false negatives, while keeping true positives and true negatives as high as possible. In this work we consider a *positive* to be an aggregator detected as deviator, and a *negative* an aggregator classified as benign.

As explained in previous sections, the idea is that manipulating behaviour will stand out, as it exerts a larger or smaller influence in other aggregators allocations, compared to the scenario’s average. Formally, one can use the normalised difference matrix  $\bar{d}$  defined in the previous section in order to quantify this mathematically: manipulating behaviour from aggregator  $i$  towards aggregator  $j$  is translated into a too large or too small entry  $\bar{d}^{i,j}$ . We propose applying a threshold-based algorithm, with threshold parameter  $\alpha$ , as described in Algorithm 1. In more detail, the algorithm looks at the difference matrix  $\bar{d}$ , computes the medians of the matrix entries, and then finds the entry that deviates the most from the median. This is done separately for off- and on-diagonal elements (as there are intrinsic magnitude differences between  $\bar{d}^{i,i}$  and  $\bar{d}^{i,j}$  even when all aggregators are benign) and only the highest deviation of the two is taken as final candidate. Lastly, this candidate is classified as deviator if its deviation from the median is greater than the user-chosen threshold  $\alpha$ .

The choice of threshold  $\alpha$  is critical and we empirically study the performance of different thresholds in Section 7.4. Also, although the presented algorithm is designed to work in scenarios with at most one manipulating agent, by selecting the aggregator that deviates the most, it can be easily adapted to a general scenario. The most straightforward way would be to simply classify as deviator any aggregator  $i$  with  $|\mu_{1/2} - \bar{d}^{i,j}| > \alpha$  for some  $j$ . This extended algorithm is conceptually the same as Algorithm 1 and will be studied in future work.

```

Input :  $\bar{d}, \alpha$ 
Output: list with the detected manipulating aggregator, if any

/* off-diagonal */
consider the off-diagonal elements: offDiag;
compute the median:  $\mu_{1/2} = \text{median}(\text{offDiag})$ ;
compute distances from each element in offDiag to  $\mu_{1/2}$ ;
find max distance  $\rightarrow$  maxOffDiag;

/* on-diagonal */
consider the on-diagonal elements: onDiag;
compute the median:  $\mu_{1/2} = \text{median}(\text{onDiag})$ ;
compute distances from each element in onDiag to  $\mu_{1/2}$ ;
find max distance  $\rightarrow$  maxOnDiag;

/* threshold-based detection */
max(maxOffDiag, maxOnDiag)  $\rightarrow$  max;
aggregator index: index(max)  $\rightarrow$  i;
if max >  $\alpha$  then
    | deviator  $\rightarrow$  [i];
else
    | deviator  $\rightarrow$  [];
end

return deviator

```

**Algorithm 1:** Threshold-based strategic manipulation detection algorithm for a scenario with at most one deviator.

We are now ready to present an empirical evaluation in order to test the performance of the decentralised algorithm proposed in Section 4.4 and the manipulation detection algorithm presented in this section.

## 7. Empirical Evaluation

In this section we present an analysis of the performance of the decentralised algorithm proposed in Section 4.4 and of the manipulation detection framework specified in Section 5. This empirical evaluation uses real market and vehicle usage data from Spain. We will

start by detailing the real data employed in the simulations, and then describe the empirical results.

### 7.1 Experimental Setup

The experiment setup described in this section closely follows the case studies presented in (Perez-Diaz et al., 2018b, 2018c, 2018a). We consider a night-time residential scenario in which EVs arrive in the evening and need to be charged by the next morning. The EVs are assumed to be medium-sized with 24kWh battery capacity and maximum charging speed  $P_{\max} = 3.7\text{kW}$ . Moreover, charging efficiency is set to 90%.

Real market data from the Spanish day-ahead market OMIE<sup>1</sup> is used in the simulations, as described in (Perez-Diaz et al., 2018b). Specifically, for this paper we focus on trading data from the November 2016. Similarly, real driver data from a Spanish survey is used to determine probabilistic EV driving patterns, as detailed in (Perez-Diaz et al., 2018b). In more detail, we employ the distribution of times for the first and last trip from and to home, as shown in Table 3.

$t_0$	Time	19h	20h	21h	22h	23h
	Probability	0.16	0.25	0.32	0.12	0.15
$t_d$	Time	6h	7h	8h	9h	10h
	Probability	0.04	0.02	0.34	0.5	0.1

Table 3: Possible arrival ( $t_0$ ) and departure ( $t_d$ ) times rounded to the nearest hour, with their respective probabilities.

Regarding energy requirements, the desired state of charge of an EV at arrival and departure times are drawn from uniform distributions as follows:  $\text{SoC}_0 \in [\text{SoC}_{\text{total}}/4, \text{SoC}_{\text{total}}/2]$  and  $\text{SoC}_f \in [2 \cdot \text{SoC}_{\text{total}}/3, \text{SoC}_{\text{total}}]$ . Consequently, the EV charging requirements range between a large percentage of the battery (up to 75%), to a small percentage (down to 16%), accounting for long and short trips home.

### 7.2 Convergence Results

We start our experimental analysis by considering the convergence to the optimal solution of the proposed decentralised algorithm without any manipulation. A key determinant of convergence is the augmented Lagrangian parameter  $\rho$  (see Eqs. (7a), (7b), (7c)). Intuitively, it controls the *weight* that the similarity of local and global solutions has in the local minimisation algorithms (see Eq. 7a). If it is set too large or too small, the algorithm will not converge. For every problem, there is a range of values providing convergence, but again, for some values it can be very slow. Also, the number of participating aggregators affects the convergence of the algorithm: the higher the number of participants, the more fragmented the optimisation problem is, so more iterations may be required. Thus, a suitable value for  $\rho$  needs to be found in order to make the algorithm converge fast, a key point for its practical applicability.

---

1. <http://www.omie.es/en/inicio>

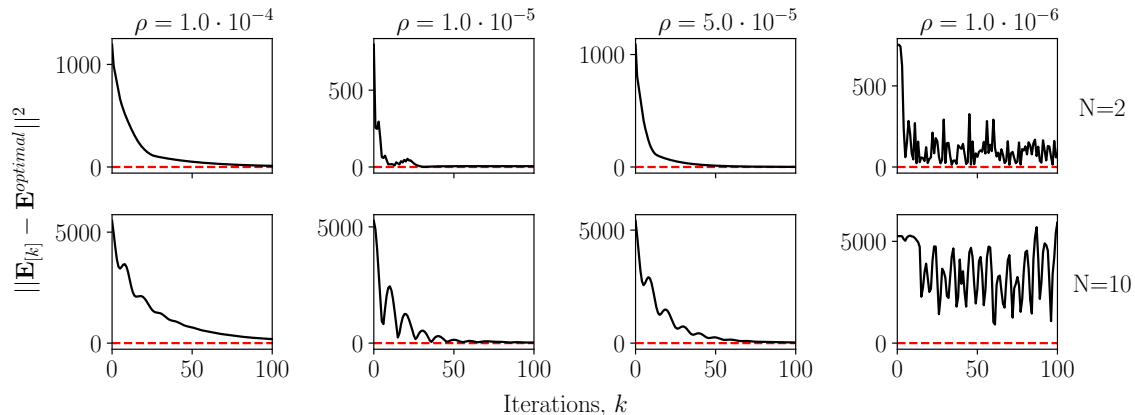


Figure 6: Convergence of the ADMM decentralised algorithm to the optimal centralised solution, for different values of  $\rho$ . (Top) Simulations with two aggregators, each with 150 000 EVs. (Bottom) Simulations with ten aggregators, each with 150 000 EVs. Market data from 1/11/2016.

Fig. 6 shows the convergence for different values of  $\rho$ , and for two scenarios, with two and ten EV aggregators respectively. Each plot shows how far the decentralised solution is from the optimal solution. We can see similar convergence behaviour for the two scenarios, although the case with two EV aggregators is faster and more uniform. These results show evidence of good computational scaling with the number of EV aggregators, something key for tackling larger problem sizes. Moreover, for both scenarios, convergence starts slow for a value of  $\rho = 10^{-3}$ , becoming fastest for a value  $\rho \sim 10^{-5}$ , and diverging for larger values. This suggests that a value about  $\rho = 10^{-5}$  presents the best convergence for these scenarios, although this may vary for larger problem sizes. Also, we would like to note that these results are consistent across different trading days. Lastly, there are novel extensions of the ADMM algorithm which include an adaptive parameter  $\rho$  and can provide faster convergence and rule out the need for parameter tweaking (Xu, Figueiredo, & Goldstein, 2017).

### 7.3 Difference Matrix Normalisation Results

As described in Section 6.1, the *difference matrix*,  $d$ , includes natural deviations arising from size differences between aggregators. Any detection algorithm employing this matrix would present higher accuracy if these differences are flattened, as any discrepancies would then come from manipulating behaviour and would clearly stand out. Therefore, we seek a way to normalise the matrix  $d$  in order to eliminate, or at least minimise, these natural differences.

In order to do so, extensive simulations were performed, studying a variety of scenarios with different number of aggregators of different sizes, and different attacks and attack strengths, which are summarised in Table 4. Then, we empirically tested different normalisation approaches. The best results were achieved by employing the normalisation given by Eq. 11 in Section 6.1. An example of the normalisation effects is pictured in Fig. 7. In this

plot, the effect of the manipulating aggregator is shown in light grey, whereas the rest of the dark grey bars correspond to benign behaviour. In the top plots, corresponding to the *difference matrix*  $d$ , we can see large differences between different entries, arising from the large size differences between the aggregators. Importantly, these natural differences are larger than the effect of the manipulating aggregator. On the contrary, the normalised bottom plots manage to nearly flatten all the natural differences, and the effect of the deviator aggregator clearly stands out.

Although we present one example, this effect is consistent and found in all the studied simulations. Further research to justify this normalisation theoretically and potentially improve it is left for future work.

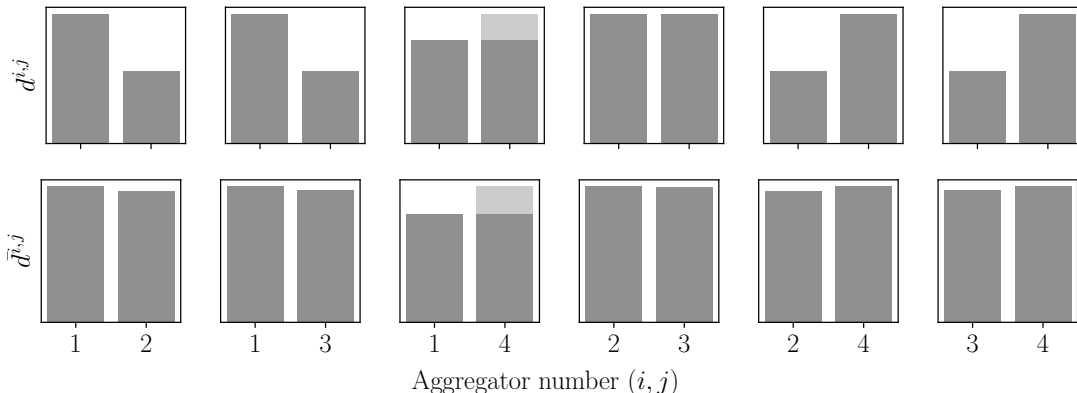


Figure 7: *Difference matrix* (top) and *normalised difference matrix* (bottom),  $d$  and  $\bar{d}$  respectively, for a scenario with two aggregators of size 50 000 EVs and two aggregators of size 150 000 EVs. One of the small aggregators (Aggregator 4) performs a displacement attack with  $\mu = 1$  against the other small aggregator (Aggregator 1), displayed as light grey.

#### 7.4 Threshold-Based Detection Results

As mentioned in Section 6.2, the choice of parameter  $\alpha$  is critical for the usefulness of the proposed threshold-based detection algorithm. In this section we will study this issue and find suitable values for  $\alpha$ . Recall that the ultimate aim is to maximise correct classifications, *i.e.* true positives and true negatives. If  $\alpha$  is set too high, we will fail to detect deviating behaviour. Conversely, if  $\alpha$  is set too low, the detection algorithm would be too sensitive and misclassify benign aggregators as manipulating.

Classical tools for carrying out this type of threshold analysis include *receiver operating characteristic* (ROC) curves and *accuracy* analysis (Metz, 1978). Formally, a ROC curve plots false positive rate (FP) versus true positive rate (TP) for each value of the threshold  $\alpha$ . An ideal algorithm would present a curve passing through  $FP = 0$  and  $TP = 1$ . Conversely, a random algorithm would lie on the line of slope 1. The results for Algorithm 1 for each type of attack are depicted in Fig. 8, using the simulations described in Table 4. We can see that the adversarial attacks are easier to detect, followed by the displacement attacks.

Proportional attacks are the most challenging, specially when the attack strength  $\lambda$  is small. However, the weaker the attack, the more limited influence it has on the convergence of the algorithm. Also, note that the ROC curves do not go all the way up to 1 TP as we focus on scenarios with at most one manipulator in this work (see Section 6.1).

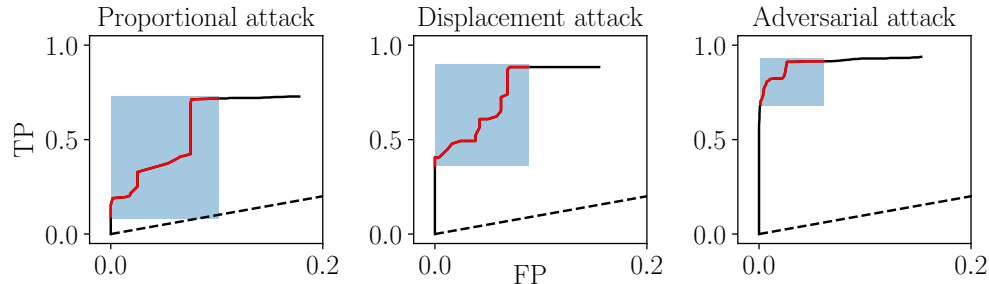


Figure 8: ROC curves for Algorithm 1 for each attack type. The dashed line corresponds to the unit slope line, where a random algorithm would lie. The highlighted areas correspond to the range of values of  $\alpha$  which provide the best results:  $\alpha \in [0.0006, 0.0356]$ . Note that these highlighted areas correspond to the highlighted areas in Fig. 8.

Moreover, we also analyse the *accuracy* (Metz, 1978) of the detection algorithm, which is given by:

$$Accuracy = \frac{True\ Positives + True\ Negatives}{Total\ population}$$

The results for Algorithm 1 for each type of attack are depicted in Fig. 9. We can see that, for all three types of attack, the proposed algorithm achieves high accuracy rates, up to around 96%, and down to around 90%, for values of  $\alpha$  in the range  $\alpha \in [0.0006, 0.0356]$ . This range is pictured in Figs. 8 and 9 with greyed areas.

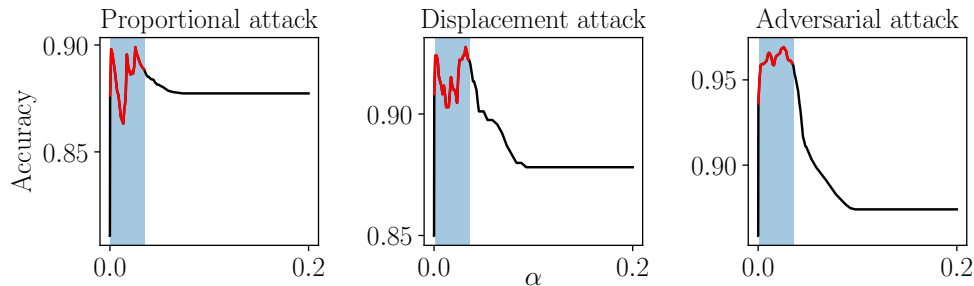


Figure 9: Accuracy curves for Algorithm 1 for each attack type. Recall that accuracy is defined as:  $Accuracy = (True\ Positives + True\ Negatives) / Total\ population$ . The highlighted areas correspond to the range of values of  $\alpha$  that provides best accuracy results:  $\alpha \in [0.0006, 0.0356]$ . Note that these highlighted areas correspond to the highlighted areas in Fig. 8.

	Attack magnitude	Number of aggs.	Size of aggs.
Proportional attack	$n = 3, 4, 6$ $\rho = 10^{-5}$ days = 10 size = 150k $\lambda = 0, 0.15, 0.3,$ 0.46, 0.61, 0.77, 0.92	$n = 3, 4, 5, 6, 7$ $\rho = 10^{-5}$ days = 10 size = 150k $\lambda = 0.5$	Aggregators= [100k, 150k, 100k], [100k, 150k, 150k], [150k, 150k, 100k], [150k, 150k, 50k], [50k, 150k, 150k], [50k, 150k, 50k], [100k, 150k, 100k, 100k], [50k, 150k, 150k, 50k] days = 10 $\lambda = 0.25, 0.5$
Displacement attack	$n = 3, 4, 5$ $\rho = 10^{-5}$ days = 2 size = 150k, $\mu = 1, 2, 3$	$n = 3, 4, 5, 6, 7$ $\rho = 10^{-5}$ days = 5 size = 150k $\mu = 1$	Aggregators= [100k, 150k, 100k], [150k, 150k, 50k], [50k, 150k, 150k], [50k, 150k, 50k], [150k, 150k, 150k, 50k], [50k, 150k, 150k, 50k] days = 2 $\mu = 1, 2$
Adversarial attack	$n = 3, 4, 5$ $\rho = 10^{-5}$ days = 10 size = 150k $\lambda = 0, 0.16, 0.33,$ 0.5, 0.66, 0.83, 1	$n = 3, 4, 5, 6, 7$ $\rho = 10^{-5}$ days = 10 size = 150k $\lambda = 0.5$	Aggregators= [100k, 150k, 100k], [100k, 150k, 100k], [150k, 150k, 100k], [150k, 150k, 50k], [50k, 150k, 150k], [50k, 150k, 50k], [150k, 150k, 150k, 50k], [50k, 150k, 150k, 50k] days = 10 $\lambda = 0.5$

Table 4: Description of all the simulations employed in the case study, Sections 7.3 and 7.4, separated by attack type.  $n$  is the number of aggregators,  $\rho$  is the augmented Lagrangian parameter,  $days$  is the number of trading days employed,  $size$  is the number of EVs per aggregator. In all cases, simulations were run twice: first with all benign aggregators, and second where the last aggregator deviates and attacks the first aggregator.

## 8. Conclusion

In this paper, we present a decentralised coordination mechanism for multi-EV aggregator bidding in the day-ahead market, employing an Alternating Direction Method of Multipliers

(ADMM) algorithm. This proposed algorithm extends previous work in the literature, which addresses the same scenario, but with a centralised framework. Specifically, the proposed decentralised framework removes the need for the aggregators to communicate private requirement information to the coordinator, as each aggregator solves its own local private optimisation problem with their own requirements. This is a key feature for the practical applicability of the proposed coordination mechanism, as real businesses or public service providers would be reluctant to disclose this private information.

Also, we present the first study about strategic manipulation of ADMM algorithms by self-interested internal agents. ADMM and related decentralised optimisation algorithms are widely applied in many disciplines, but little work has focused on studying how this algorithms can be disrupted by internal attackers. In this paper, we introduce three attacks that a self-interested aggregator can employ in order to alter the outcome of the ADMM algorithm for its own benefit. Also, we detail a mathematical framework which measures the effects that different agents exert onto each other when employing the ADMM algorithm, and propose a detection which detects manipulating behaviour, *i.e.* participants that do not adhere to the vanilla ADMM algorithm and try to cheat the system. Although we focus on an energy setting, the proposed detection framework is general and can be applied to any ADMM setting.

In order to study the proposed algorithm and detection mechanism, we present an empirical evaluation using real market and vehicle usage data from Spain. We first show the convergence of the decentralised method to the optimal solution for two scenarios, with two and ten cooperating EV aggregators respectively. Convergence can be achieved in around 50 iterations in the first case and around 80 in the second case. Therefore, although problem complexity increases with the number of participants, these numbers suggest the applicability of the algorithm in large settings. With respect to the threshold-based detection algorithm, we present ROC and accuracy analyses in order to study detection capabilities with different thresholds  $\alpha$ . We find good detection accuracy, up to 96% for most attacks, and down to 90% in some cases, showing that the algorithm is able to correctly identify deviations in most cases.

Several aspects are left for future work. First, a more thorough analysis of the effects of each of the proposed attack types on the algorithm’s outcome and its convergence would shed more light on effective attack vectors. Secondly, studying how the detection algorithm can be improved and extended further than scenarios with at most one potential deviator would provide increased practical applicability. Thirdly, studying the proposed framework in a general ADMM formulation, rather than our energy setting, may provide generalised insights into the resilience of the algorithm.

## Acknowledgements

This work was supported by an EPSRC (UK) Doctoral Training Centre grant (EP/L015382/1).

## References

Ardakanian, O., Keshav, S., & Rosenberg, C. (2014). Real-Time Distributed Control for Smart Electric Vehicle Chargers: From a Static to a Dynamic Study. *IEEE Transac-*



- tions on *Smart Grid*, 5(5), 2295–2305.
- Bessa, R. J., & Matos, M. A. (2013a). Global against divided optimization for the participation of an EV aggregator in the day-ahead electricity market. Part I: Theory. *Electric Power Systems Research*, 95, 309–318.
- Bessa, R. J., & Matos, M. A. (2013b). Global against divided optimization for the participation of an EV aggregator in the day-ahead electricity market. Part II: Numerical analysis. *Electric Power Systems Research*, 95, 309–318.
- Bessa, R. J., Matos, M. A., Soares, F. J., & Lopes, J. A. P. (2012). Optimized bidding of a EV aggregation agent in the electricity market. *IEEE Transactions on Smart Grid*, 3(1), 443–452.
- Boyd, S., Parikh, N., Chu, E., Peleato, B., & Eckstein, J. (2010). Distributed Optimization and Statistical Learning via the Alternating Direction Method of Multipliers. *Foundations and Trends in Machine Learning*, 3(1), 1–122.
- Chen, Y., Kar, S., & Moura, J. M. (2018). Resilient Distributed Estimation Through Adversary Detection. *IEEE Transactions on Signal Processing*, 66(9), 2455–2469.
- Gan, L., Topcu, U., & Low, S. H. (2013). Optimal Decentralized Protocols for Electric Vehicle Charging. *IEEE Transactions on Power Systems*, 28(2), 940–951.
- Gonzalez Vaya, M., & Andersson, G. (2015). Optimal Bidding Strategy of a Plug-In Electric Vehicle Aggregator in Day-Ahead Electricity Markets Under Uncertainty. *IEEE Transactions on Power Systems*, 30(5), 2375–2385.
- Herranz, R., Muñoz San Roque, A., Villar, J., & Campos, F. A. (2012). Optimal demand-side bidding strategies in electricity spot markets. *IEEE Transactions on Power Systems*, 27(3), 1204–1213.
- International Energy Agency (2016). Global EV Outlook 2016: Beyond one million electric cars. Tech. rep..
- International Energy Agency (2017). Global EV Outlook 2017: Two million and counting. Tech. rep..
- Kempton, W., Tomic, J., Letendre, S., Brooks, A., & Lipman, T. (2001). Vehicle-to-Grid Power: Battery, Hybrid, and Fuel Cell Vehicles as Resources for Distributed Electric Power in California. *Fuel Cell, IUCD-ITS-R*(June), 95.
- Le Floch, C., Belletti, F., & Moura, S. (2016). Optimal Charging of Electric Vehicles for Load Shaping: A Dual-Splitting Framework With Explicit Convergence Bounds. *IEEE Transactions on Transportation Electrification*, 2(2), 190–199.
- Le Floch, C., Belletti, F., Saxena, S., Bayen, A. M., & Moura, S. (2015). Distributed optimal charging of electric vehicles for demand response and load shaping. *Proceedings of the IEEE Conference on Decision and Control*, 54rd IEEE(Cdc), 6570–6576.
- Liao, M., & Chakraborty, A. (2016). A Round-Robin ADMM algorithm for identifying data-manipulators in power system estimation. *Proceedings of the American Control Conference*, 2016-July, 3539–3544.

- Liao, M., & Chakraborty, A. (2017). Identifying data-manipulators in power system mode estimation loops with noisy measurements. *Proceedings of the American Control Conference*, pp. 2773–2778.
- Liao, M., & Chakraborty, A. (2018). Optimization Algorithms for Catching Data Manipulators in Power System Estimation Loops. *IEEE Transactions on Control Systems Technology*, 1–16.
- Ma, Z. J., Callaway, D. S., & Hiskens, I. A. (2013). Decentralized Charging Control of Large Populations of Plug-in Electric Vehicles. *Ieee Transactions on Control Systems Technology*, 21(1), 67–78.
- Metz, C. E. (1978). Basic principles of ROC analysis.. *Seminars in Nuclear Medicine*, 8(4), 283–298.
- Mukherjee, J. C., & Gupta, A. (2017). Distributed Charge Scheduling of Plug-In Electric Vehicles Using Inter-Aggregator Collaboration. *IEEE Transactions on Smart Grid*, 8(1), 331–341.
- Munsing, E., Mather, J., & Moura, S. (2017). Blockchains for decentralized optimization of energy resources in microgrid networks. *2017 IEEE Conference on Control Technology and Applications (CCTA)*, 2164–2171.
- Munsing, E., & Moura, S. (2018). Cybersecurity in Distributed and Fully-Decentralized Optimization: Distortions, Noise Injection, and ADMM..
- Peng, Q., & Low, S. H. (2014). Distributed algorithm for optimal power flow on a radial network. In *53rd IEEE Conference on Decision and Control*, pp. 167–172.
- Perez-Diaz, A., Gerding, E., & McGroarty, F. (2018a). Decentralised Coordination of Electric Vehicle Aggregators. In *International Workshop on Optimization in Multiagent Systems (OptMAS-18)*, pp. 1–15.
- Perez-Diaz, A., Gerding, E. H., & McGroarty, F. (2018b). Coordination and payment mechanisms for electric vehicle aggregators. *Applied Energy*, 212, 185–195.
- Perez-Diaz, A., Gerding, E. H., & McGroarty, F. (2018c). Coordination of Electric Vehicle Aggregators: A Coalitional Approach. In *Proc. of the 17th International Conference on Autonomous Agents and Multiagent Systems (AAMAS 2018)*.
- Qi, W., Xu, Z., Shen, Z. J. M., Hu, Z., & Song, Y. (2014). Hierarchical coordinated control of plug-in electric vehicles charging in multifamily dwellings. *IEEE Transactions on Smart Grid*, 5(3), 1465–1474.
- Rigas, E. S., Ramchurn, S. D., & Bassiliades, N. (2015). Managing Electric Vehicles in the Smart Grid Using Artificial Intelligence : A Survey. *Ieee Transactions on Intelligent Transportation Systems*, 16(4), 1619–1635.
- Scott, P., & Thiébaux, S. (2014). Dynamic Optimal Power Flow in Microgrids using the Alternating Direction Method of Multipliers. *CoRR*, 1–8.
- Shao, C., Wang, X., Wang, X., Du, C., & Wang, B. (2016). Hierarchical Charge Control of Large Populations of EVs. *IEEE Transactions on Smart Grid*, 7(2), 1147–1155.

- Sulc, P., Backhaus, S., & Chertkov, M. (2014). Optimal Distributed Control of Reactive Power Via the Alternating Direction Method of Multipliers. *IEEE Transactions on Energy Conversion*, 29(4), 968–977.
- Wang, Y., Wu, L., & Wang, S. (2017). A Fully-Decentralized Consensus-Based ADMM Approach for DC-OPF with Demand Response. *IEEE Transactions on Smart Grid*, 8(6), 2637–2647.
- Wen, C.-k., Chen, J.-c., Teng, J.-h., & Member, S. (2012). Decentralized Plug-in Electric Vehicle Charging Selection Algorithm in Power Systems. *IEEE Intelligent Systems*, 3(4), 1779–1789.
- Wu, H., Shahidehpour, M., Alabdulwahab, A. S., & Abusorrah, A. (2016). A Game Theoretic Approach to Risk-Based Optimal Bidding Strategies for Electric Vehicle Aggregators in Electricity Markets With Variable Wind Energy Resources. *IEEE Transactions on Sustainable Energy*, 7(January), 118.
- Xu, Z., Figueiredo, M. A. T., & Goldstein, T. (2017). Adaptive ADMM with Spectral Penalty Parameter Selection. In *Proceedings of the 20th International Conference on Artificial Intelligence and Statistics (PMLR)*, Vol. 54, pp. 718–727.
- Yu, J. J. Q., Lin, J., Lam, A. Y. S., & Li, V. O. K. (2016). Maximizing Aggregator Profit through Energy Trading by Coordinated Electric Vehicle Charging. In *IEEE International Conference on Smart Grid Communications (SmartGridComm)*.